



Fermi National Accelerator Laboratory

FERMILAB-Conf-90/201

SUPERFLIC—A Recirculating Superconducting Linear Collider Toponium Factory *

J. B. Rosenzweig
Fermi National Accelerator Laboratory
P.O. Box 500
Batavia, Illinois 60510

October 1, 1990

* Submitted to the proceedings of the 1st Workshop on a TeV Superconducting Linear Collider, Ithaca, New York, July 23-26, 1990.



Operated by Universities Research Association Inc. under contract with the United States Department of Energy

SUPERFLIC – A Recirculating Superconducting Linear Collider Toponium Factory *

J.B. Rosenzweig
Fermi National Accelerator Laboratory
P. O. Box 500, Batavia, Illinois 60510

October 1, 1990

Abstract

The conceptual design of a 0.3-0.4 TeV e^+e^- linear collider which uses superconducting RF (SRF) accelerating cavities is presented. This machine is intended to provide high luminosity and low collision energy spread to allow precise studies of the $t\bar{t}$ resonant states. Only through use of SRF is such a collider made possible. It features use of recirculation arcs as a partial remedy to presently low SRF accelerating gradients. Development of this type of collider is motivated by and could serve as a stepping stone to exploiting SRF at higher energies. In TeV-range SRF colliders the serious difficulties arising from the beam-beam interaction, very small beam sizes and tolerances characteristic of normal conducting machines can be greatly diminished.

*Submitted to the Proceedings of the 1st TeV Superconducting Linear Accelerator (TESLA) Collider Workshop, held at Cornell University, July 23-26, 1990.

Introduction

The future of high-energy e^+e^- collider physics in the post-LEP era undoubtedly resides with linear colliders [1]-[3]. The considerable research effort aimed towards a proposable linear collider design – a TeV linear collider (TLC) – has concentrated on schemes using normal conducting accelerating structures. As it seems likely that a first proposal, from SLAC and/or KEK, for an intermediate energy linear collider (ILC - 0.5 TeV in the center-of-mass) will appear within a few years, it is imperative that any challenge to this standard approach be mounted within a very short time. The object of the 1st TeV Superconducting Linear Accelerator (TESLA) Workshop held at Cornell in July, 1990, was to discuss the option of a TeV linear collider using superconducting RF (SRF) structures. The potentially dramatic advantages of SRF for use in a linear collider have been documented in the recent past[5][6], but given that the accelerating gradient reliably achieved to date in operating SRF cavities is less than 10 MV/m, the superconducting approach has not been taken seriously as a contender for the next generation of linear collider.

The purpose of this paper is to propose a scheme which SRF to be considered as a viable option for a linear collider with only modest improvements in the performance of superconducting cavities. This scheme uses a recirculation arc (the last gasp of the circular machines!) to effectively double the accelerating gradient. It is proposed to use this machine to attain intermediate energy (0.3-0.4 TeV) e^+e^- collisions for precision studies of the toponium system, with the precise energy of course determined by the as yet unmeasured top quark mass[7]. Putting forward this design serves the purposes of both studying a realistic option for the next generation of high-energy physics experimentation and to bring SRF into active consideration for use in this and other future linear colliders.

The fact that a toponium factory cannot be built using room temperature accelerating structures without prohibitively high power use makes the SRF option even more attractive. A toponium factory that can resolve the mass differences of excited states of the $t\bar{t}$ system requires that the spread in collision energies due to beamstrahlung energy loss be less than approximately one GeV[7]. As will be seen below, this can be accomplished at required luminosities using SRF by colliding intense bunches ($N \geq 3 \times 10^{10}$) at high frequency ($f_c \sim 10$ kHz), while keeping total power use small through the

much higher efficiency of the superconducting approach. This philosophy can be exploited at high energy, also, allowing design of a 1.5 TeV center-of-mass linear collider which completely avoids the serious problem of coherent pair production from the beam-beam interaction[8][9].

Advantages of Superconducting RF

The advantages of superconducting RF are at first glance manifold, but they all find their root in the increased efficiency of wall to beam power conversion. The inherent inefficiency of pulsed normal conducting travelling wave structures affects all of the issues which concern the design of a linear collider. The pressing issues surrounding implementation of the normal conducting approach are numerous, and have been researched extensively [3]-[4]. These schemes grew out of an evolutionary philosophy in which existing linear collider (*i.e.* SLC) concepts and technologies are extrapolated in hopes of reaching the desired energies and luminosities. This process, despite claims that it is a conservative effort, leads to unfavorable design constraints which undermine the credibility of the proposed colliders. As efficiency and cost considerations necessitate use of higher RF frequencies[2, 4], these constraints include potentially serious problems from beam loading, single and multi-bunch beam breakup (BBU), and development of affordable pulsed RF (millimeter wave) peak power in the range 100 MW or greater. The most troubling issues, however, surround the final focus, at which the vertical beam size is envisioned to be on the order of a few nanometers. The problems associated with beamstrahlung energy loss and pair creation[8] in normal conducting schemes result in severe constraints on the design of the final focus and beam-crossing region. In addition, the need for such strong focusing introduces uncontrollable chromatic aberrations through synchrotron radiation in the final quadrupoles (the Oide effect[10]), which limits the beam height to be greater than approximately a nanometer. Perhaps the most daunting extrapolation of existing techniques is the operational need to align, focus and bring into collision two beams of nanometer height without a proven scheme for diagnosing beam properties of these dimensions.

Many of the implications of these constraints can be seen qualitatively from examining expressions concerning the luminosity, as well as disruption

and beamstrahlung effects in a linear collider. The luminosity is given by

$$\mathcal{L} = \frac{f_c N^2}{4\pi\sigma_x\sigma_y},$$

where $\sigma_x\sigma_y$ is the transverse spot size. Note that luminosity scales as $N\bar{I}$, where $\bar{I} = Ne f_c$ is the average beam current. If power conversion efficiency is too low, then the only way to reach luminosities on the order of $\mathcal{L} = 10^{33} (\text{E(TeV)})^{-2}$ is to focus the beam spot down to the range $\sigma_x\sigma_y \simeq 100 \text{ nm}^2$. This constraint can be mitigated considerably by use of SRF, as the wall plug to beam power conversion efficiency in an optimized design can be expected to be approximately 25%. This is a factor of at least 5 larger than for a normal conducting design. As approximately one-half of the power consumption for an optimized SRF linear collider is in the cryogenic system, the actual beam current $\bar{I} = V/P_b$ can be an order of magnitude larger in the SRF designs.

The disruption parameter D is a measure of the number of betatron oscillations a particle undergoes as it passes through the focusing fields generated by the oncoming beam during collision. This focusing effect is beneficial in a linear collider, as enhanced luminosity and relaxed collision alignment tolerances result, but only to a point ($D \lesssim 15$) where the effects of the kink instability becomes begin to degrade luminosity performance[11]. For asymmetric gaussian beams, the disruption parameter in each plane is given by

$$D_{x,y} = \frac{2Nr_e\sigma_z}{\gamma\sigma_{x,y}(\sigma_x + \sigma_y)}.$$

For very flat beams ($R = \sigma_x/\sigma_y \gg 1$), the larger vertical disruption parameter is lowered by a factor of $R/2$ over the equivalent round beam.

It would appear that to keep the disruption parameter to a manageable level one need only shorten the bunch length σ_z . Aside from technical difficulties associated with creating very short bunches this is not desirable from the point of view of beamstrahlung energy loss. The fractional energy loss due to beamstrahlung (fractional spread in collision energies) is

$$\delta \simeq (8/9) \frac{r_e^3 N^2 \gamma}{\sigma_z \sigma_y^2 (1 + R)^2} H(\Upsilon)$$

where the σ_z^{-1} dependence reflects the fact that the peak beam-beam force

scales inversely with the bunch length. The factor

$$H(\Upsilon) \simeq \frac{1}{(1 + (4/3)\Upsilon^{2/3})^2}$$

accounts for quantum corrections to the classical radiation formula, where

$$\Upsilon \equiv \frac{E_c}{E} \simeq \frac{5r_e^2 N \gamma}{12\pi \sigma_z \sigma_y (1 + R)}$$

is the ratio of the synchrotron radiation critical energy to the beam energy. Thus to suppress the beamstrahlung energy loss it is highly desirable to have larger beam sizes in all dimensions at collision. This is possible if one can afford large average beam currents and/or bunch sizes.

The performance of a collider for HEP experimentation may be limited by the collision energy spread, especially in the case of a precision machine like a $t\bar{t}$ factory. It may also be limited by the related problem of background generation due to coherent pair production. The number of pairs per beam crossing is approximately (including only the contribution from real photons and assuming $\Upsilon \ll 1$)[8]

$$N_{e^+e^-} \simeq 0.044N \left[\frac{\alpha \sigma_z}{\gamma \lambda_c} \Upsilon \right]^2 \exp[-16/3\Upsilon].$$

Note the dominant Υ dependence of this process. These pairs can have much smaller energy than the primary beam particles, and one of the pair will be defocused rather than focused in the field of the oncoming beam, causing it to be ejected out towards the detector. This forms a serious concern about backgrounds. Chen and Telnov have made arguments that some pair creation is inevitable due to the incoherent scattering of beamstrahlung photons and thus one does not have to suppress the coherent process entirely, but merely make its contribution smaller than that from the incoherent process. In the TeV collision range the conclusion reached from suppressing the coherent pair production entirely requires about a factor of two smaller Υ than from this prescription. Thus requiring $N_{e^+e^-} < 1$, which implies $\Upsilon \lesssim 0.2$, gives a practical rule for suppressing coherent pair production with a safety factor included.

This discussion illustrates that diminishing of the deleterious coherent beam-beam processes requires beams larger in all dimensions. The normal

conducting approach, however, requires small transverse beam sizes – to achieve the required luminosity with lower N and \bar{I} and small bunch lengths ($\sigma_z \ll 1$ mm, due both to the requirement $\sigma_z < \beta_y^* \simeq 100\mu\text{m}$ and from operation at short RF wavelengths, $\lambda = 1\text{-}2.5$ mm). Amelioration of coherent beam-beam effects in the normal conducting scheme requires multibunching schemes which introduce new complications due to BBU and crossing instabilities. Through the efficient operation with higher beam currents at longer RF wavelengths, SRF permits access of higher energy collisions, with smaller energy spreads and diminished coherent pair production problems from beamstrahlung.

There are additional operational advantages to use of lower RF frequency and larger beams at collision. The lower RF frequency reduces the coupling of the beam to both transverse and longitudinal wake-fields, by a factor of ω^3 and ω^2 , respectively. This scaling, in addition to the much more open, smooth apertures allowed in a standing wave SRF accelerating structure, makes control of energy spread and single and multibunch BBU much more straightforward. The necessary damping of higher order modes to control multibunch BBU can be accomplished with much less intrusive couplers (every 5-10 cells[5] instead of every cell[4]) in the SRF approach. In addition, because of the smaller coupling of the beam to wake-fields, it need not be focused as strongly in the linac to provide BNS damping. Larger beam sizes imply that the final focus is less demanding (the Oide effect does not enter into consideration, the momentum acceptance is larger) and much larger emittances can be used. Since the tolerances on vibration and alignment are proportional to the beam size in the linac, larger emittances and weaker focusing imply easing of these tolerances. The tolerances are of the order 10 nm (vibration) and 50 μm (alignment) for normal conducting TLC-type schemes, so this advantage is of considerable importance.

Design of a Superconducting RF Linear Collider

The most complete treatment of the physics issues in linear collider design and the subsequent optimization of design parameters for TLC-type (normal conducting 0.5-1.5 TeV) colliders has been compiled by Palmer[4]. The ap-

proach employed here relies heavily on Palmer's perceptive statement of the problem and the formulae he uses to analyze the design issues. Although the superconducting approach is quite different than the tack Palmer takes, much of what is needed to discuss the SRF linear collider design is contained in his work. Rather than repeat all of the extensive body of relevant results obtained from Ref. [4], the reader is referred to that paper for many of the details of the design constraints employed below.

There have also been a number of published analyses of the specific design problems associated with a SRF linear collider. The present effort is based to some extent on the previous by work Padamsee[2], Rubin[5] and Sundelin[6], where issues specific to SRF have been identified. A shared conclusion of these works is that for achieved Q -values of a few times 10^9 that the collider must run in a pulsed mode with a few percent duty cycle to prevent excessive dissipation of rf power at cryogenic temperatures. The designs presented here also operate in this regime, but differ from those previously presented in added reliance on raising the average beam current. This naturally leads to questions about the feasibility of generating large fluxes of cooled electrons and positrons. A somewhat detailed sketch of damping rings which can provide the necessary cold beams is included below, which is based in large part on Sands' monograph on electron storage rings[12] with some help from Ref. [4]. The damping rings are quite large (containing hundreds of bunches) and have fast damping times in order to meet the requirements on the needed currents and emittances. The emittances required are in general over an order of magnitude larger than specified for normal conducting designs. This opens the door to doing away with the electron damping ring entirely, as the requisite beam brightness and emittances may be obtained directly from an RF photocathode source[13].

The additional difference in the designs presented here from others is in the emphasis on use of recirculation arcs to effectively double the accelerating gradient obtained for a given capital investment in linac. This scheme also permits more efficient power use, in that the power overhead associated with dumping the stored energy in the cavities and the static heat leak of the cryostats is halved. As the gradients reliably attained in SRF cavities are still under 10 MV/m, the recirculation arc, which is conceptually inspired by both CEBAF and SLC[14], can be viewed as a fast way to jump into contention for the next generation of linear collider. Two different design parameters corresponding to two possible collision energies, $150 + 150$ and

200 + 200 GeV[7], are presented to show the scheme's usefulness and also its limitations in this energy range. At energies higher than 100 GeV (half the total energy) the energy loss and/or emittance growth in the arcs quickly becomes intolerable.

The conceptual development of the recirculating superconducting toponium factory has an additional *raison d'être*: that of exploring the possibilities for entry into the lepton physics arena by Fermilab. Thus the somewhat whimsical acronym *SUPERFLIC* – *SUPER*conducting *F*ermilab *L*inear Collider. This work is being performed under the aegis of a long range planning group, and as such is a very preliminary exploration. Beyond the interesting HEP experimentation which can be done at a toponium factory, two aspects of the concept are particularly attractive. First, there is a tradition of successfully applying superconducting technology to HEP accelerators at Fermilab. Also, the recirculation arcs make the machine compact enough to possibly fit on the existing Fermilab site. This concern should not, however, be overestimated, as the concept should not be considered site specific. Rather, this effort is primarily an attempt to stir interest in more research and development of SRF for linear collider applications, which can be performed anywhere there is interest – Cornell, CERN, SLAC, DESY, CEBAF, Wuppertal, etc.

SUPERFLIC Design Parameters

In order to make the multidimensional space of linear collider design parameters with their complicated interrelations manageable, a spread sheet program has been employed. This program, unlike Palmer's, is only a passive calculator and does not perform optimization of parameters automatically. The optimization is performed by iteration after inspection of the full parameter lists, which takes time but has the positive effect of requiring that some insight be gained into the design constraints. Also, in contrast to Palmer's treatment, no dilution factors in emittances or intensities are included in the calculation. Rather, the philosophy adopted here is to over-design by large safety factors, so that there is much slack in the performance of the collider as designed.

The collider under discussion is shown schematically in Figure 1. There are two linacs of length L_{acc} connected end-to-beginning by recirculation arcs.

Bunches of $e^-(e^+)$ starting at injection energies (damping ring $E \simeq 1.5$ GeV) accelerate through the linacs towards the $e^+(e^-)$ bunches accelerating in the opposing linac. The bunches at approximately half of their final energy are then bent outward into the recirculation arcs. The arcs are composed of two sections, a gentle bend consisting of two portions with equal but opposite radius of curvature ρ_1 , and a more severe, smaller radius of curvature ρ_2 , π -bend before reinjection into the opposing linac. After specifying ρ_2 and the distance between the ends of the linac and the interaction point L_{IP} , one finds

$$\rho_1 = \frac{[(L_{acc}/2) + L_{IP}]^2 + \rho_2^2}{2\rho_2},$$

and a total bend angle in the first section of

$$\psi = 2 \arcsin([(L_{acc}/2) + L_{IP}]/\rho_1).$$

The actual radii of curvature ρ inside of the arc dipoles are larger by a factor of f_p^{-1} , the inverse of the dipole packing fraction. The beams suffer a non-negligible energy loss traversing the arcs. For an isomagnetic section of bend the fractional energy loss is given by[14]

$$\frac{\Delta E}{E_0} = 1 - (1 + 3\alpha_e \psi)^{-1/3}$$

where $\alpha_e = 8.85 \times 10^{-5} E_0^3 (\text{GeV}^3)/2\pi\rho(\text{m})$, and E_0 is the beam energy at the beginning of the bend. This quantity becomes unbearably large (> 0.1) for the types of bends considered here as the energy is raised much past 100 GeV.

The other issue of overriding concern in the arcs is that of horizontal emittance blowup. Following the example of the SLC arcs (a combined function FODO lattice) the normalized rms emittance growth in a section of bend is given by

$$\Delta\epsilon_{n,x} = 4.1 \times 10^{-8} \psi \frac{E_0^6}{f_p \rho} \langle H/\rho \rangle$$

where the lattice dependent quantity

$$\langle H/\rho \rangle = \langle (\gamma\eta^2 + 2\alpha\eta\eta' + \beta\eta'^2)/\rho \rangle.$$

Assuming $\rho \propto E_0$, the emittance growth has an E_0^4 dependence, which is even more severe than the relative energy loss. For the SLC arcs the phase advance per cell was taken to be 108 degrees and [14] and

$$\langle H/\rho \rangle \simeq 1.65 \left(\frac{l_c}{2\rho} \right)^3 ;$$

thus the cell length l_c should be chosen as small as possible (limited by available field gradient) to minimize emittance growth. In the interest of simplicity, the designs presented here for the recirculation arcs are based on a scaling of the SLC arcs. More complicated lattices that yield smaller emittance growth should also be considered, but this is outside the scope of the present work. Calculated emittance growth using the SLC scheme is adequate for the present purposes. The normalized vertical emittance growth due to radiation antidamping in the arcs is in the 10^{-8} m-rad level, and thus has negligible effects on the design.

The design parameters for two different example versions of SUPER-FLIC, one with 150+150 GeV energy and an accelerating gradient of 30 MeV/m, and another with 200+200 GeV energy and accelerating gradient of 40 MeV/m, are calculated by the spread sheet program and organized into numbered pages:

1. The first page lists the characteristics of the beam and final focus. The input parameters are beam energy, accelerating gradient E_{acc} , number of particles per pulse N , average beam collision rate f_c , bunch length σ_z , normalized emittances ϵ_n , final beta-functions β^* , bunch separation in linac and final quad pole tip field. From these quantities, characteristics of the final focus and the beam-beam interaction are derived. These include: the beam sizes at collision σ^* , the disruption parameters D , angles and enhancement H_D , the momentum bandwidth of the final focus, the beamstrahlung energy spread δ , parameter Υ and number of expected coherent pairs produced, and the luminosity.
2. Page two contains the design parameters for a continuous wiggler damping ring [15]. Input parameters include energy E_d , peak field in the wiggler magnets, horizontal partition function J_x , horizontal betatron tune ν_x , bunch spacing $\Delta\tau_b$, dipole packing fraction, bunch length σ_d , number of bunches n_d and the ratio harmonic number h to n_d . The derived

parameters include the average ring radius, β -function and dispersion η , from which we estimate $\langle H/\rho \rangle$. Input parameters N and f_c are taken from page one. Also calculated are synchrotron energy loss per turn, the damping times in both planes, and the number of damping times until extraction. The critical radiation energy, equilibrium emittances and energy spread are listed. Derived parameters related to the RF system and the longitudinal dynamics are RF voltage, frequency and synchronous phase, synchrotron tune, and bunch and bucket area in phase space. Maximum allowed ring impedance Z/n for beam stability, and vacuum vessel power dissipation load are also given.

3. The third page concerns the power parameters describing the performance of the SRF linacs. Input of a rough geometrical description of the RF system is done by specifying cell aperture, length, number of cells per cavity frequency ω , Q , and shunt impedance per unit length R_s/Q . The cryogenic system inputs are cryo temperature, refrigerator efficiency, static heat leak rate, and the fraction of beam excited higher order mode (HOM) power dissipated at cryo temperature. Also specified are the klystron efficiency and cavity fill time. Input parameters N and f_c are taken from page one, and number of bunches per RF pulse (same as the number of bunches in the damping rings) from page two. Derived parameters include the HOM loss factor, beam-loaded Q_l , peak and matched RF power requirements, RF rep rate, pulse length and duty cycle, and effective power dumping time. The total power consumption, consisting of RF power into the beam and dumped and the end of the pulse divided by klystron efficiency, plus the cryogenic power, the fundamental and HOM power dissipated in the superconducting walls divided by the carnot and refrigerator efficiencies. The total wall plug and beam powers, as well as the efficiency are listed.
4. Page four describes the recirculation arcs. The energy E_0 , magnetic radius of the π -bend (section 2), FODO cell length l_c , phase advance per cell and dipole packing fraction are input. Derived parameters include length and radius of the initial (section 1) bends, the growth of the emittances and energy spread due to quantum emission of synchrotron radiation, and the total energy loss around the arcs.
5. Page five gives some parameters related to alignment and vibration

tolerances. We specify the focusing characteristics by the phase advance per cell, quad packing fraction and the field gradient. The geometrical description of the cavities input from page three allows estimation of the longitudinal and transverse wake functions. With the bunch intensity, bunch length and focusing scheme, the expected energy spread from wake-fields and the induced correlated energy spread necessary for BNS damping can be calculated. The total number of quads encountered, the chromatic betatron phase spread and the beam sizes then are used to derive vibration and alignment tolerances.

6. Page six represents a weak attempt at estimating a cost for a SUPER-FLIC project, including only the capital cost of the machines and the electrical running costs. The cost estimates on this page (which should be self-explanatory), are based partly on Sundelin's treatment[6], rough extrapolations of completed or current projects, and on presentations at the TESLA workshop. This page is included only to give an idea of costs; these will be known better *only* after cavity development has advanced.

This listing only enumerates the parameters that are input and calculated and to some extent how they are related. A close look at the example designs that have been arrived at is much more instructive in illustrating the design constraints and comparisons to normal conducting linear colliders.

Concentrating for the moment on the 150+150 GeV collider example, we see that the luminosity has been chosen to be $\mathcal{L} = 1.3 \times 10^{33} \text{ cm}^{-2}\text{s}^{-1}$. The assumed accelerating gradient is 30 MV/m, giving an linac length of about 2.5 km. In the spirit of the workshop, the emittances and β^* 's were chosen to give somewhat arbitrarily $\sigma_y^* = 100 \text{ nm}$ (two orders of magnitude larger than TLC and ILC-like designs) and $\sigma_x^* = 1 \mu\text{m}$. The horizontal emittance and σ_x^* are almost identical to SLC design parameters. The final vertical beam size, while as yet unprecedented, will soon be attempted at the SLAC Final Focus Test Facility[16]. The bunch length is chosen to be $\sigma_z = 0.5 \text{ mm}$ (still an order of magnitude longer than normal conducting schemes) to give a large (2 mrad) diagonal angle $\theta_d = \sigma_x/\sigma_z$. Once the beam dimensions are chosen, the maximum number of particles per bunch consistent with a fractional energy loss $\delta = 0.66 \%$ is taken, $N = 3 \times 10^{10}$. The desired luminosity is then attained by setting the collision frequency to 10 kHz. The bunch separation of 2 μsec (1 μsec when the bunches interleave after the arcs, to be compared with

about a nsec separation for normal conducting multi-bunch designs[4]) in the linac is chosen to give multibunch beam stability as calculated for reasonable HOM Q 's by Rubin[5]. The disruption parameter and enhancement are quite modest, $D_y = 2.6$ and $H_D = 1.81$, so there is no problem with kink instability and the design luminosity is not strongly dependent on the beam-beam effect. The maximum disruption angle θ_m for these parameters is 0.43 mrad. The beam crossing angle is chosen to be $\theta_c = \sqrt{\theta_m \theta_d} = 0.93$ mrad, precluding the complication of a crab-crossing scheme[17]; the beam 'exhaust' can be made to miss the final optical elements through use of this crossing angle without significant loss in luminosity. The momentum acceptance of the final focus is calculated from the general arguments due to K. Brown[4], and is found to be much larger than the expected momentum spread. The final β -functions are much larger than the bunch length. If the focusing of submicron beams develops further, β_y^* can be reduced to be equal to σ_z to raise the luminosity to $\mathcal{L} = 2.3 \times 10^{33} \text{ cm}^{-2}\text{s}^{-1}$. This is accomplished at essentially no penalty, as the beamstrahlung energy loss and maximum disruption angle depend very weakly on the beam height when $R \gg 1$.

The damping ring energy is chosen to balance fast damping with the effects of quantum emission of synchrotron radiation, which blow up the energy spread and horizontal emittance, to be 1.5 GeV. The dipole field in the wigglers (1.7 T) and the dipole packing fraction (0.6) are chosen for due to similar constraints. A minimum bunch spacing based on the limits of extraction/injection kicker technology is chosen to be 30 nsec. To make the total pulse length large to the RF dumping time, we chose $n_d = 200$ bunches per ring. Thus the ring must have an average radius of 286 m, which is quite a bit larger than an ILC-type ring, which has an order of magnitude fewer bunches. The betatron tune is chosen to be fairly high to minimize $\langle H/\rho \rangle$ (and the equilibrium horizontal emittance), but not so high that the average dispersion and the momentum compaction become unacceptably low. Small dispersion implies a lot of sextupole correction for the chromaticity, which can lead to a small dynamic aperture in the ring. The equilibrium normalized emittances are about $\epsilon_{n,x} = 12 \text{ mm-mrad}$ and $\epsilon_{n,y} = 0.01 \text{ mm-mrad}$, well below those ($\epsilon_{n,x} = 50 \text{ mm-mrad}$ and $\epsilon_{n,y} = 1 \text{ mm-mrad}$) specified for the final focus. Since we have chosen $J_x = 2.5$, the horizontal damping is 2.5 times faster than the vertical damping rate. There are 13 vertical damping times per damping ring cycle, and assuming an initial vertical emittance from the positron source is less than $5 \times 10^2 \text{ mm-mrad}$, the final emittance has

in fact equilibrated. The initial positron vertical emittance could be more than a factor of ten larger than this and still meet final focus emittance requirements with this damping ring.

The RF system of the ring is specified once the bunch length is taken to be $\sigma_z = 1.5$ cm, chosen partly to provide for a large tolerable ring impedance ($Z/n = 2.32\Omega$, an order of magnitude larger than ILC or TLC-type designs) without making the beam longitudinally unstable, but also to give a reasonable RF voltage, which here is $V = 81$ MV. This is large due to the large energy spread $\Delta E/E = 0.31$ % (also necessary for longitudinal stability) and the size of the ring radius, but must be so also to overshadow the synchrotron energy loss per turn of 8.9 MeV. These choices give a synchronous phase of $\phi_s = 6.3$ degrees. As could be anticipated, the radiated power per unit length is large, almost 800 kW/m, but this is not considerably larger than present rings must dissipate. With large RF voltage and small momentum compaction the bucket area is much larger than the equilibrium longitudinal emittance, so quantum lifetime effects are not a concern. The RF must supply the beam with 1.4 MW of power; it could be assumed that SRF cavities will be employed for the task for efficiency's sake.

The characteristics of the SRF cavities and the cryostat are very similar to Rubin's conceptual design of a TESLA collider[5], to take advantage of the design approach used and the multibunch BBU stability analysis included. The 3 GHz cavities have 10 cells to minimize the number of feeds per unit length subject to the constraint of damping the HOM Q 's sufficiently for BBU stability. The klystron efficiency is taken to be 0.6, the cavity $Q = 4 \times 10^9$ and shunt impedance $R_s/Q = 1920\Omega$, corresponding to experience with Cornell/CEBAF cavities. Only the accelerating gradient is extrapolated beyond current technology. The cavity fill time is chosen at 100 μ sec to be significantly smaller than the pulse length of 400 μ sec, and gives a peak power demand of 250 kW/m. The matched $Q_{ext} = Q_l = 3.25 \times 10^6$ yields an effective cavity power dumping time of 173 μ sec, and a matched RF power demand of 144 kW/m. These RF powers are three orders of magnitude smaller than normal conducting schemes demand. The RF rep rate is 50 Hz, which is quite similar to SLC.

The cryogenic temperature is assumed to be 2° K, with a static heat leak of 1 W/m and a refrigerator efficiency of 0.2. All sources of power dissipated at 2° K, HOM (assumed half dissipated in cavity walls) fundamental (including the filling and dumping times), and static heat leak, sum to 28

kW, which when divided by the refrigerator and Carnot efficiency gives a cryogenic power demand of 20.4 MW. The Rf power is accounted for by the beam power (14.4 MW) and the dumped power (6.2 MW). Dividing these by the klystron efficiency, one obtains total power to generate the necessary RF of 34.4 MW. Thus the total wall plug power use by the machine is only 54.8 MW and the efficiency is 26.3 %. A normal conducting machine of this energy (with $\delta < 1$ %) using 14.4 MW of stably transported beam power would use over 250 MW of wall plug power.

The recirculation arcs are specified to be at about half of the final beam energy, with a magnetic radius in section 2 of 650 m and a distance from linac to interaction point $L_{IP} = 500$ m. The dipole packing fraction is taken to be 0.9 (to save space; this also motivates the combined function FODO lattice design) and the cell length 8 m. The radii of curvature in the arcs are $\rho_1 = 2.48$ km, $\rho_2 = 0.72$ km. Almost all of the emittance growth and energy loss occur in the tighter bends of section 2 where the beams must be turned 180° around. The total energy loss is 2.29 GeV out of 75 GeV initial, and the normalized emittance blowups (which should be summed in squares with the initial emittance) are $\Delta\epsilon_{n,x} = 19.6$ and $\Delta\epsilon_{n,y} = 0.01$ mm-mrad, and so the emittances for final focus are more than adequate. It should be noted in this regard that if these vertical emittances of less than 0.1 mm-mrad can be preserved through the linac and arc, then focusing down to $\beta_y^* = \sigma_z$ gives a luminosity of $\mathcal{L} = 8.6 \times 10^{33} \text{ cm}^{-2}\text{s}^{-1}$, at a vertical beam size of $\sigma_y^* = 13$ nm, which is daunting but still an order of magnitude larger than TLC-type designs. This added luminosity again comes without penalty in beamstrahlung energy loss.

The alignments and tolerances are calculated from the specified focusing scheme in the linacs, a $\psi = 90^\circ$ phase advance per cell FODO lattice, which provides a β -function scaled like $\gamma^{1/2}$ in the first pass through the linacs. During the second pass through the phase advance per cell is not constant and is less than 90° . The maximum transverse and longitudinal wake-fields are obtained from the geometric specifications of the cavities and the bunch length. From these considerations and the β -function in the linac the necessary correlated energy spread for BNS damping of single bunch BBU is found to be 0.16%; this spread is removed at the end of acceleration. The final corrected (by optimizing bunch placement on the accelerating wave) energy spread from both the arcs and the longitudinal wake-fields is 0.06 %, well inside the final focus bandwidth. The vertical alignment tolerance from

consideration of chromatic focusing effects is given by[18]

$$\Delta_y = \frac{\sigma_f}{\psi(\delta p/p)} \sqrt{\frac{2}{N_q}}$$

where σ_f is the final beam size in the linac and N_q is the total number of focusing elements encountered by the beams. This gives a vertical alignment tolerance of 1.2 mm, as opposed to about 33 μm for a typical ILC design[4]. The tolerances on vibration of optical elements are more stringent, and these are given for our focusing scheme by[18]

$$\Delta_y \simeq \sigma_f \sqrt{\frac{3}{8N_q}}.$$

This yields a vertical vibration tolerance of 0.4 μm , which is small unless one compares it to the 12 nm tolerances required for a typical ILC design. These improvements in tolerances are permitted almost entirely due to larger beam sizes in the linac, mostly from relaxation of the emittance requirements but partly due to easing of required energy spread and focusing needed for BNS damping.

Another, related, source of tolerance requirements comes from transverse kicks arising from asymmetries in the accelerating cavities from couplers, field emission currents, and construction errors. Any asymmetries of this sort which change on a pulse-to-pulse basis give rise to tolerance requirements similar to the vibration tolerances. Since the SRF cavities have fewer HOM couplers per unit length, and less coupling of the beam to phenomena occurring near the wall, it can be assumed that these concerns are greatly diminished in SRF designs.

In the particular case of SUPERFLIC, however, the arcs present a source of additional path length which is fairly strongly focused to minimize the horizontal emittance growth. This gives rise to slightly tighter tolerances than the alternative case of linacs which are twice as long, due to the encountering of additional optical elements during acceleration. This is not, however, a serious consideration.

The cost of these colliders is estimated in a rudimentary way, assuming costs which scale only in proportion to with the length of the components of the machine. The cost per active meter of the linacs is estimated to be \$125 k (less than CEBAF, higher than TESLA goals[2]), of the damping rings

(only one is assumed necessary) to be \$30 k, and of the arcs, which have no RF, to be \$15 k. The capital cost for construction is about \$770 M, and the electrical operating cost integrated over four years is \$150 M. Note that in this estimation use of the recirculation arcs save approximately \$430 M in capital cost, and about \$40 M in electrical operating cost. These estimates are not unreasonable, but are fundamentally guesses; if and when the SRF cavities are developed, the rest of design follows and only then can a reliable cost estimate be ventured. If higher accelerating gradients are possible in SRF linacs, however, one can state with confidence that for a fraction of the cost of the SSC a well-defined physics goal may be achievable with a SRF linear collider.

The second design at 200+200 GeV is given in Appendix 2. In order to boost the luminosity to $\mathcal{L} = 2.35 \times 10^{33} \text{ cm}^{-2}\text{s}^{-1}$ without additional beamstrahlung energy spread, more beam charge $N = 4 \times 10^{10}$, the bunch is made longer $\sigma_z = 0.75 \text{ mm}$ and wider $\sigma_x = 1.5 \mu\text{m}$, but the beam height is reduced to 67 nm. The fractional energy loss $\delta = 0.53 \%$ is actually smaller in this case. To keep the size of the machine approximately the same an accelerating gradient of 40 MV/m is assumed. The additional beam charge and energy leads to a raising of the beam power to 25.6 MW, so even though the conversion efficiency of the machine is higher (27.4 %) the total wall plug power is 93.5 MW. In most respects the scaling of this machine is straightforward, except for the recirculation arcs. The energy loss in the arcs is now 6 %, and the horizontal emittance growth is twice as large. Extrapolation of this type of machine beyond 250+250 GeV (125 GeV arcs) is not attractive. Removal of the arcs yields not too dissimilar, but more expensive, designs of the type discussed in Ref. [9].

Conclusions

Several aspects of this design study are specific to the recirculating linac. The arcs can allow a significant cost savings which may be used to permit SRF to be more seriously considered for the next generation of linear collider, which it can be argued should be built to do precision studies of the toponium system, a mission to which an SRF linear collider is well suited. The downside of the arcs is the added complexity, emittance growth and slightly more stringent tolerances due to the extra length of beam-line.

The size of the machines, and therefore the accelerating gradient, used in this study is biased towards something which approximately fits inside of the Fermilab site. This is of course an unnecessary constraint, which upon removal permits accelerating gradients as low as 20 MV/m to be seriously considered for the recirculating toponium factory. In this case the recirculation arcs are not so big compared to the linac, and their design can be relaxed somewhat, while still keeping the energy loss and emittance growth tolerable. A design based on 20 MV/m accelerating fields gives higher efficiency but a larger capital cost (\$1.1 G). Toponium factory designs using SRF at 20 MV/m are presented in Ref. [9].

The state of research and development of high field SRF cavities shows much promise[19]. In the last decade multipacting limits have been understood and circumvented. Recently, high surface electric fields have been observed in nonaccelerating cavities at Cornell (145 MV/m)[20] and Argonne (210 MV/m)[21], which are above the level (~ 100 MV/m) expected in an accelerating cavity which is limited by the critical surface magnetic field for niobium. This limit corresponds to an accelerating field of about 50 MV/m, which is more than adequate for TeV-range linear collider applications. Present obstacles include thermal breakdown, which can be controlled by use of higher purity superconducting material, and more seriously, loading due to field emission. This effect is diminished by eliminating surface defects and contamination, which is the subject of much current investigation. Rigorous chemical and heat treatments and RF processing have yielded peak surface fields in single cell accelerating cavities of over 50 MV/m with $Q > 10^9$ in tests at Cornell[20]. Much of the recent progress in SRF is summarized in the report of the high field working group from the TESLA workshop (these proceedings) and in Ref. [19].

It would appear, then, that the required accelerating fields for development of linear colliders like those described above are tantalizingly close to realization. Further research is necessary, and any new efforts (and hopefully successes) would be timely. If the SRF technology can be made viable for the next generation of linear colliders, much further development will be necessary to exploit the advantages offered by the SRF option at and above the TeV collision energy. In total these advantages make the extrapolation to the next generation of lepton collider a proposition which requires small improvements in producing and manipulating low emittance intense beams, instead of orders of magnitude that are called for in the normal conducting

approach. The multitude of serious obstacles in linear colliders are reduced to one by SRF, that of obtaining high gradients. It is hoped that the designs presented here serve to stimulate further efforts towards making SRF linear colliders a real option for future high energy physics experimentation.

The author would like to thank those at the TESLA workshop who critiqued this work, especially Bill Barletta. The author also wishes to thank Fred Mills, Gerry Jackson, Gerry Dugan, and Steve Peggs for helpful comments. Particular thanks go to Mike Harrison for brain-storming sessions, motivation and support.

References

- [1] U. Amaldi, "Attaining Superhigh Energies With e^+e^- Collisions", pp. 295-316 *Techniques and Concepts of High-Energy Physics V*, Ed. Thomas Ferbel, NATO ASI Series B – Vol. 204, Plenum, London (1990), and "Introduction to the Next Generation of Linear Colliders", p. 341 *Frontiers of Particle Beams*, M. Month and S. Turner, Eds., Springer-Verlag, Berlin (1988).
- [2] *Proceedings of the Capri Workshop on Linear Colliders*, Eds. L. Palumbo, S. Tazzari, V.G. Vaccaro, INFN-Frascati, 1989 (note in particular H. Padamsee's article on SRF linear colliders).
- [3] *Proceedings of the International Workshop on Next-Generation Linear Colliders*, SLAC-Report-335, 1988.
- [4] R.B. Palmer, "Prospects for High Energy e^+e^- Linear Colliders", SLAC-PUB-5195, March 1990, submitted to *Annual Review of Nuclear and Particle Science*.
- [5] D. Rubin, "Superconducting RF Linear Collider", *Proceedings of the 1989 IEEE Particle Accelerator Conference*, Eds. F. Bennett and J. Kopta, p. 721, IEEE (1990).
- [6] R. Sundelin, "Superconducting RF for Direct Acceleration in TeV Colliders", *Proceedings of the 1988 Linac Conference*, 221, CEBAF-Report-89-001.
- [7] U. Amaldi, presented at 1st TESLA Workshop, Cornell, July 1990.
- [8] P. Chen and V. Telnov, *Phys. Rev. Lett.* **63**, 1796 (1989).
- [9] J.B. Rosenzweig, "Design Parameters for TeV Superconducting Linear Accelerator (TESLA) Colliders," these proceedings.
- [10] K. Oide, *Phys. Rev. Lett.* **61**, 1713 (1988).
- [11] P. Chen and K. Yokoya, *Phys. Rev. D* **38**, 987 (1988); and "Disruption effects from the interaction of flat e^+e^- beams" submitted to *Phys. Rev. D*.

- [12] M. Sands, "The Physics of Electron Storage Rings – An Introduction", 1970, available from National Technical Information Service.
- [13] J.B. Rosenzweig, "Low Emittance Flat-beam RF Photocathode Electron Source for Linear Collider Applications", these proceedings.
- [14] S. Kheifets, T. Fieguth, K.L. Brown, A. Chao, J.J. Murray, R.V. Sevrancx, and H. Wiedemann, "Beam Optical Design and Studies of the SLC Arcs", p. 168, *Proceedings of the 1989 IEEE Particle Accelerator Conference*, Eds. F. Bennett and J. Kopta, IEEE (1990).
- [15] R.B. Palmer "Cooling Rings for TeV Colliders", in *New Techniques for Future Accelerators*, Ed. M. Puglisi, et al., Plenum Physical Sciences Series V. 29 p. 121 (New York 1987).
- [16] K. Oide "Design of Optics for the Final Focus Test Beam at SLAC" *Proceedings of the 1989 IEEE Particle Accelerator Conference*, Eds. F. Bennett and J. Kopta, p. 1319, IEEE (1990).
- [17] R.B. Palmer, SLAC-PUB-4707 (1988).
- [18] R. Ruth "Emittance Preservation in Linear Colliders", in *Frontiers of Particle Beams*, Springer-Verlag Lecture Notes in Physics **296**, p. 440 (Berlin 1988).
- [19] *Proceedings of the 4th Workshop on RF Superconductivity*, Ed. Y. Kojima, KEK Report 89-21 (1989).
- [20] Q. Shu, J. Graber, W. Hartung, J. Kirchgessner, D. Moffat, R. Nower, H. Padamsee, D. Rubin, J. Sears, "Novel Approaches for Attaining High Accelerating Fields in Superconducting Cavities", Cornell Report CLNS-90/1005 (1990), see also related articles in Ref. [19].
- [21] J.R. Delayen and K.W. Shepard, "Tests of a superconducting rf quadrupole device," *Appl. Phys. Lett.* **57**, 514 (1990).

SUPERFLIC - Collider Parameters

Input Parameters - Beam and Final Focus

Beam Energy	150	GeV
Accelerating Gradient	30	MeV/m
Acceleration Length	2.5	km
Number e ⁺ /pulse	3E+10	
Beam Collision Rate	10,000	Hz
Bunch length	0.0005	m
Normalized Horizontal Emittance	4.9E-05	m-rad
Normalized Vertical Emittance	9.8E-07	m-rad
Horizontal Beta*	0.006	m
Vertical Beta*	0.003	m
Bunch Separation in Linac	2E-06	s
Final Quad Pole Tip Field	1	T

Derived Beam and Final Focus Parameters

Horizontal Beam Size at Focus	1000	nm
Vertical Beam Size at Focus	100	nm
Horizontal Disruption Parameter	0.26	
Vertical Disruption Parameter	2.60	
Disruption Enhancement	1.81	
Maximum Horizontal Disruption Angle	0.43	mrاد
Horizontal Diagonal Angle	2.00	mrاد
Horizontal Crossing Angle	0.93	mrاد
Energy Bandwidth of Final Focus	0.97%	
Beamstrahlung Parameter	0.03	
Fractional Energy Loss	0.66%	
Number of Coherent Pairs per Collision	0	

Luminosity	1.29E+33	cm⁽⁻²⁾-Hz
-------------------	-----------------	-----------------------------

Input Parameters - Damping Ring

Energy	1.5 GeV
Dipole Field in Wiggler Magnets	1.7 T
Partition Function Jx	2.5
Horizontal Betatron Tune	32
Bunch Spacing	30 nsec
Fraction of Ring in Dipoles	0.6
Bunch Length	1.5 cm
Number of Bunches	200
Harmonic Number/Number of Bunches	2

Derived Damping Ring Parameters

Average Horizontal Beta	8.95 m
Average Horizontal Dispersion	0.28 m
Average Radius	286.478 m
Horizontal Damping Time	0.64 msec
Number of Horizontal Damping Times	31
Vertical Damping Time	1.60 msec
Number of Vertical Damping Times	13
Critical Energy	4282.01 eV
Normalized Horizontal Emittance	11.77 mm-mrad
Normalized Vertical Emittance	0.01 mm-mrad
Rms Energy Spread	4.67 MeV
Relative Rms Energy Spread	0.31%
Momentum Compaction	0.00098
Synchrotron Tune	0.05785
Synchrotron Energy Loss/Turn	8.90 MeV
Total Radiated Synchrotron Power	1.42 MW
Radiated Power/ Meter	791 W/m
RF Volts/turn	81.24 MV
Maximum Ring Impedance Z/n	2.32 Ohm
RF Frequency	66.67 MHz
Synchronous Phase	6.29 Degrees
Rms Phase Spread in Bunches	1.20 Degrees
Bucket Area	7.03 eV-sec
Equilibrium Longitudinal Emittance	0.00733 eV-sec

Appendix 1 - 150 GeV Design

Input Parameters - Power

RF Cell Aperture	2	cm
Number Cells/ Cavity	10	
Assumed Klystron Efficiency	0.6	
Cryogenic Temperature	2	K
Assumed Refrigerator Efficiency	0.2	
RF Frequency	3	GHz
RF Cell Length	4	cm
Static Heat Leak	1	W/m
Fraction HOM Power at Cryo. Temp.	0.5	
Cavity Q	4E+09	
Cavity Shunt Impedance R/Q	1920	Ohm/m
Cavity Fill Time	100	usec

Derived Power Parameters

HOM Loss Factor	8.10	V/pC/m
RF Duty Cycle	0.02	
Beam Loaded Cavity QL	3255208	
Peak RF Power	249	kW/m
Matched RF Power	144	kW/m
RF Repetition Rate	50	Hz
Effective Cavity Power Dumping Time	173	usec
RF Pulse Length	400	usec
Average Beam Current	48	uA
Peak Beam Current	1152	A
Total Beam Power	14.40	MW
Dumped RF Power	6.22	MW
Carnot Efficiency	0.00683	
Fundamental Power at Cryogenic Temp	18.24	kW
HOM Power at Cryogenic Temp	4.67	kW
Static Heat Leak at Cryogenic Temp	5.00	kW
Total Refrigerator Power	20.44	MW
Total RF Power	34.36	MW

Total Wall Plug Power for Linacs	54.81	MW
Beam/Wall Plug Power Efficiency	26.27%	

Appendix 1 - 150 GeV Design

Recirculation Arcs -Input Parameters

Energy	75 GeV
Magnetic Radius Section 2	0.65 km
Cell Length	8 m
Phase Advance Per Cell	108 degrees
Bend Dipole Packing Fraction	0.9
Linac to IP Distance	0.5 km

Derived Arc Parameters

<H(s)> Section 1	2.1E-05 m
Length in Bends Section 1	3496 m
Average Radius Section 1	2.48 km
Bend Angle Section 1	1.57 rad
Radiated Energy Section 1	0.28 GeV
Critical Energy Section 1	380671 eV
Rms Quantum Energy Section 1	242977 eV
Rate of Quantum Emission Section 1	1.6E+09 Hz
Induced Rms Energy Spread Section 1	0.00047
Norm. Horiz. Emittance Blowup Section 1	0.68 mm-mrad
Norm. Vert. Emittance Blowup Section 1	0.03134 mm-mrad
Power Per Unit Length Section 1	3.83 W/m
<H(s)> Section 2	0.00031 m
Average Radius Section 2	0.72 km
Length in Bends Section 2	2042 m
Radiated Energy Section 2	2.01 GeV
Critical Energy Section 2	1437006 eV
Rms Quantum Energy Section 2	917219 eV
Rate of Quantum Emission Section 2	4.2E+08 Hz
Induced Rms Energy Spread Section 2	0.00081
Norm. Horiz. Emittance Blowup Section 2	19.60 mm-mrad
Norm. Vert. Emittance Blowup Section 2	0.06243 mm-mrad
Power Per Unit Length Section 2	47.22 W/m
Total Norm. Horizontal Emittance Blowup	19.61 mm-mrad
Total Norm. Vertical Emittance Blowup	0.09377 mm-mrad
Total Induced Energy Spread	0.09%
Total Energy Loss	2.29 GeV

Alignments and Tolerances - Input Parameters

Quadrupole Aperture	4.3 cm
Phase Advance per Cell	90 degrees
Quad Pole Tip Field	1 T
Fraction of Linac in Quads	0.01

Derived Alignment and Tolerance Parameters

Maximum Transverse Wake	41 kV/nC/m ²
Maximum Longitudinal Wake	14 kV/nC/m
Initial Linac Beta Function	7 m
Initial Quad Focal Length	7.80 m
Initial Cell Half-Length	11.03 m
Final Quad Focal Length	99 m
Final Cell Half-Length	55 m
Final Linac Beta Function	196 m
Final Uncorrected Energy Spread	0.22%
Final Corrected Energy Spread	0.05%
Initial Energy Spread for BNS Damping	0.08%
Number of Focusing Elements	1451
Chromatic Betatron Phase Spread	0.21 rad
Vertical Alignment Tolerance	1.18 mm
Horizontal Alignment Tolerance	8.30 mm
Vertical Vibration Tolerance	0.41 μ m
Horizontal Vibration Tolerance	2.90 μ m

Appendix 1 - 150 GeV Design

Input Parameters - Cost

Cost/Active meter - Linac Structure	80	k\$/m
Cost/Active meter - Refrigeration	20	k\$/m
Cost/Active meter - RF	25	k\$/m
Cost/meter - Arcs	15	k\$/m
Cost/meter - Damping Rings	30	k\$/m
Number of Damping Rings	1	
Electricity Cost	0.08	\$/kW-hr
Integrated Running Time	4	years

Derived Power Parameters

Linac Cost	625	M\$
Arc Cost	92	M\$
Damping Ring Cost	54	M\$

Capital Cost	771	M\$
Operating Cost	154	M\$
Project Cost	925	M\$

SUPERFLIC - Collider Parameters

Input Parameters - Beam and Final Focus

Beam Energy	200	GeV
Accelerating Gradient	40	MeV/m
Acceleration Length	2.5	km
Number e ⁺ -/pulse	4E+10	
Beam Collision Rate	10,000	Hz
Bunch length	0.00075	m
Normalized Horizontal Emittance	4.9E-05	m-rad
Normalized Vertical Emittance	4.9E-07	m-rad
Horizontal Beta*	0.018	m
Vertical Beta*	0.00356	m
Bunch Separation in Linac	2E-06	s
Final Quad Pole Tip Field	1	T

Derived Beam and Final Focus Parameters

Horizontal Beam Size at Focus	1500	nm
Vertical Beam Size at Focus	67	nm
Horizontal Disruption Parameter	0.18	
Vertical Disruption Parameter	4.11	
Disruption Enhancement	1.85	
Maximum Horizontal Disruption Angle	0.29	mrاد
Horizontal Diagonal Angle	2.00	mrاد
Horizontal Crossing Angle	0.76	mrاد
Energy Bandwidth of Final Focus	1.22%	
Beamstrahlung Parameter	0.03	
Fractional Energy Loss	0.53%	
Number of Coherent Pairs per Collision	0	

Luminosity	2.35E+33	cm⁽⁻²⁾-Hz
-------------------	-----------------	-----------------------------

Appendix 2 - 200 GeV Design

Input Parameters - Damping Ring

Energy	1.5 GeV
Dipole Field in Wiggler Magnets	1.7 T
Partition Function Jx	2.5
Horizontal Betatron Tune	32
Bunch Spacing	30 nsec
Fraction of Ring in Dipoles	0.6
Bunch Length	1.5 cm
Number of Bunches	200
Harmonic Number/Number of Bunches	2

Derived Damping Ring Parameters

Average Horizontal Beta	8.95 m
Average Horizontal Dispersion	0.28 m
Average Radius	286.478 m
Horizontal Damping Time	0.64 msec
Number of Horizontal Damping Times	31
Vertical Damping Time	1.60 msec
Number of Vertical Damping Times	13
Critical Energy	4282.01 eV
Normalized Horizontal Emittance	11.77 mm-mrad
Normalized Vertical Emittance	0.01 mm-mrad
Rms Energy Spread	4.67 MeV
Relative Rms Energy Spread	0.31%
Momentum Compaction	0.00098
Synchrotron Tune	0.05785
Synchrotron Energy Loss/Turn	8.90 MeV
Total Radiated Synchrotron Power	1.90 MW
Radiated Power/ Meter	1055 W/m
RF Volts/turn	81.24 MV
Maximum Ring Impedance Z/n	1.74 Ohm
RF Frequency	66.67 MHz
Synchronous Phase	6.29 Degrees
Rms Phase Spread in Bunches	1.20 Degrees
Bucket Area	7.03 eV-sec
Equilibrium Longitudinal Emittance	0.00733 eV-sec

Appendix 2 - 200 GeV Design

Input Parameters - Power

RF Cell Aperture	2 cm
Number Cells/ Cavity	10
Assumed Klystron Efficiency	0.6
Cryogenic Temperature	2 K
Assumed Refrigerator Efficiency	0.2
RF Frequency	3 GHz
RF Cell Length	4 cm
Static Heat Leak	1 W/m
Fraction HOM Power at Cryo. Temp.	0.5
Cavity Q	4E+09
Cavity Shunt Impedance R/Q	1920 Ohm/m
Cavity Fill Time	100 usec

Derived Power Parameters

HOM Loss Factor	6.62 V/pC/m
RF Duty Cycle	0.02
Beam Loaded Cavity QL	3255208
Peak RF Power	442 kW/m
Matched RF Power	256 kW/m
RF Repetition Rate	50 Hz
Effective Cavity Power Dumping Time	173 usec
RF Pulse Length	400 usec
Average Beam Current	64 uA
Peak Beam Current	1024 A
Total Beam Power	25.60 MW
Dumped RF Power	11.05 MW
Carnot Efficiency	0.00683
Fundamental Power at Cryogenic Temp	32.43 kW
HOM Power at Cryogenic Temp	6.77 kW
Static Heat Leak at Cryogenic Temp	5.00 kW
Total Refrigerator Power	32.38 MW
Total RF Power	61.09 MW

Total Wall Plug Power for Linacs	93.47 MW
Beam/Wall Plug Power Efficiency	27.39%

Appendix 2 - 200 GeV Design

Recirculation Arcs -Input Parameters

Energy	100 GeV
Magnetic Radius Section 2	0.8 km
Cell Length	8 m
Phase Advance Per Cell	108 degrees
Bend Dipole Packing Fraction	0.9
Linac to IP Distance	0.5 km

Derived Arc Parameters

<H(s)> Section 1	2.8E-05 m
Length in Bends Section 1	3667 m
Average Radius Section 1	2.17 km
Bend Angle Section 1	1.88 rad
Radiated Energy Section 1	1.19 GeV
Critical Energy Section 1	1033158 eV
Rms Quantum Energy Section 1	659449 eV
Rate of Quantum Emission Section 1	5.9E+08 Hz
Induced Rms Energy Spread Section 1	0.00059
Norm. Horiz. Emittance Blowup Section 1	1.89 mm-mrad
Norm. Vert. Emittance Blowup Section 1	0.03328 mm-mrad
<H(s)> Section 2	0.0002 m
Power Per Unit Length Section 1	20.82 W/m
Average Radius Section 2	0.89 km
Length in Bends Section 2	2513 m
Radiated Energy Section 2	4.77 GeV
Critical Energy Section 2	2699737 eV
Rms Quantum Energy Section 2	1723201 eV
Rate of Quantum Emission Section 2	2.2E+08 Hz
Induced Rms Energy Spread Section 2	0.00093
Norm. Horiz. Emittance Blowup Section 2	22.62 mm-mrad
Norm. Vert. Emittance Blowup Section 2	0.0543 mm-mrad
Power Per Unit Length Section 2	121.50 W/m
Total Norm. Horizontal Emittance Blowup	22.70 mm-mrad
Total Norm. Vertical Emittance Blowup	0.08759 mm-mrad
Total Induced Energy Spread	0.11%
Total Energy Loss	5.96 GeV

Appendix 2 - 200 GeV Design

Alignments and Tolerances - Input Parameters

Quadrupole Aperture	4.3 cm
Phase Advance per Cell	90 degrees
Quad Pole Tip Field	1 T
Fraction of Linac in Quads	0.01

Derived Alignment and Tolerance Parameters

Maximum Transverse Wake	61 kV/nC/m ²
Maximum Longitudinal Wake	14 kV/nC/m
Initial Linac Beta Function	7 m
Initial Quad Focal Length	7.80 m
Initial Cell Half-Length	11.03 m
Final Quad Focal Length	127 m
Final Cell Half-Length	90 m
Final Linac Beta Function	249 m
Final Uncorrected Energy Spread	0.22%
Final Corrected Energy Spread	0.06%
Initial Energy Spread for BNS Damping	0.16%
Number of Focusing Elements	1493
Chromatic Betatron Phase Spread	0.17 rad
Vertical Alignment Tolerance	0.70 mm
Horizontal Alignment Tolerance	6.95 mm
Vertical Vibration Tolerance	0.28 μ m
Horizontal Vibration Tolerance	2.79 μ m

Appendix 2 - 200 GeV Design

Input Parameters - Cost

Cost/Active meter - Linac Structure	80	k\$/m
Cost/Active meter - Refrigeration	15	k\$/m
Cost/Active meter - RF	30	k\$/m
Cost/meter - Arcs	15	k\$/m
Cost/meter - Damping Rings	30	k\$/m
Number of Damping Rings	1	
Electricity Cost	0.08	\$/kW-hr
Integrated Running Time	4	years

Derived Power Parameters

Linac Cost	625	M\$
Arc Cost	103	M\$
Damping Ring Cost	54	M\$
Capital Cost	782	M\$
Operating Cost	262	M\$
Project Cost	1044	M\$

SUPERFLIC

SUPERconducting Fermilab Linear Collider

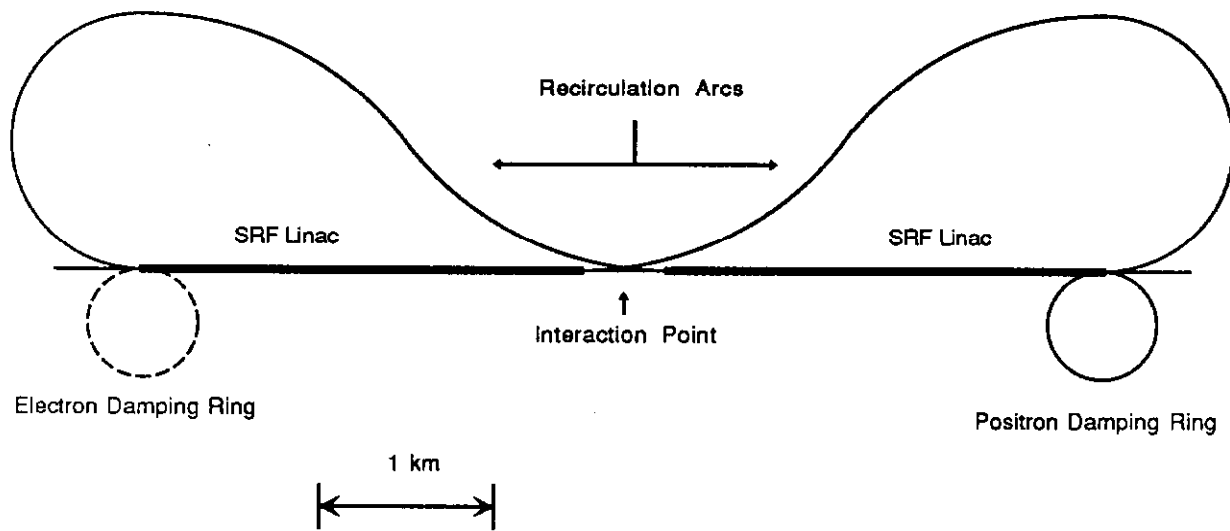


Figure 1. Schematic drawing of 150+150 GeV recirculating superconducting linear collider.

Electron damping ring may be unnecessary, due to development of low emittance RF photocathode source.